Mehran University Research Journal of Engineering and Technology

https://doi.org/10.22581/muet1982.2401.2910

2024, 43(1) 24-33

Heat transfer augmentation through engine oil-based hybrid nanofluid inside a trapezoid cavity

Muhammad Awais [a], Feroz Ahmed Soomro [b, *], Shreen El-Sapa [c], Rahim Bux Khokhar [d]

[a] *Department of Mechanical Engineering, Quaid-e-Awam University of Engineering, Science and Technology, Larkana 77150, Sindh Pakistan*

[b] *Department of Mathematics, Xiamen University Malaysia, Sepang 43900, Selangor Malaysia*

[c] *Department of Mathematical Sciences, College of Science, Princess Nourah Bint Abdulrahman University, P. O. Box 84428, Riyadh 11671, Saudi Arabia*

[d] *Department of Basic Science and Related Studies, Mehran University of Engineering and Technology, Jamshoro 76062, Sindh Pakistan*

[*] Corresponding author: Feroz Ahmed Soomro, Email: ef.ey.soomro@gmail.com

Received: 12 July 2023, Accepted: 20 December 2023, Published: 01 January 2024

K E Y W O R D S

Heat Transfer Rate

Hybrid Nanofluid

Fluid-Structure Interaction

Finite Element Method

Partial Differential Equations

A B S T R A C T

Heat transfer occurs as a result of density differences caused by temperature changes. It has several industrial applications. To improve performance, one must investigate the heat transfer behaviour of the working fluid. Hence, the purpose of this work is to report a heat transfer analysis of a partially heated trapezoid cavity filled with a hybrid nanofluid. The temperature conditions of the cavity are such that the bottom boundary is partially heated, inclined side boundaries are kept at a lower temperature, and the upper boundary is kept adiabatic. A trapezoidal shape heated obstacle is considered in the cavity's centre. The heat transfer and flow take place inside the cavity due to density variation. The mechanism is regulated by mass, momentum, and energy conservation, as well as related boundary constraints. The solutions are determined by the use of a numerical technique known as the Finite Element Method after the governing equations are transformed into non-dimensional form, which brings up physical parameters affecting the heat transfer and flow. The initial study is performed for three types of nanofluids with silver Ag and magnesium oxide Mgo nanoparticles inside water H_2O, kerosene Ke, and engine oil EO. The study revealed that the engine oil-based hybrid nanofluid produced an increased heat transfer rate. Simulation is performed using engine-based hybrid nanofluid with the range of physical parameters, such as Rayleigh number Ra $(10^5 \leq Ra \leq 10^7)$, Hartmann number Ha $(0 \leq Ha \leq 100)$ and nanoparticles volume fraction ϕ $(0 \leq \phi \leq 0.2)$. It is found that the heat transfer rate is enhanced by increasing the fraction of nanoparticles in the base fluid. Moreover, imposition of magnetic field has reverse impact on the fluid movement.

1. Introduction

Heat transfer has paramount importance in our daily life, from the human body dissipating heat to the cooling of electronic equipment, to the extraction of geothermal energy [1-2]. In order to increase the efficiency of already existing devices their heat transfer rates must be improved. Traditional fluids such as water and ethylene glycol are known to improve heat transfer rates, but because of these fluids' low thermal conductivities, they are not performing up to the requirement. In order to improve the poor thermal conductivity of these conventional base fluids a new fluid known as nanofluid has been studied widely [3-5]. The first study was carried out by Choi in 1995 and his experimental results suggest that incorporating nanosized particles (1-100 nm) with base fluids (water, air) results in high thermal conductivities of these fluids which in turn improve the heat transfer rates [6]. After that much research has been carried out using nanofluids inside various shapes (square, rectangle, rhombus, and trapezoid) cavities [7-10]. For these reasons, the study of nanofluids inside various complex-shaped geometries in the field of fluid dynamics is an area of interest nowadays.

Numerous studies have been carried out in the past, MHD natural convection numerical investigation using hybrid nanofluid inside a trapezoid cavity was performed by Mohammad et al. [11]. A study carried out by Ghalambaz et al. [12] on hybrid nanofluids inside square shaped cavity to study various physical quantities related to heat transfer study suggested incorporating nanofluids increases heat transfer rates when the Rayleigh number is low in the conduction flow regime, whereas the local Nusselt number decreases in the convection flow domain as the flow moves from bottom to top. Sreedevi and Sudarsana [13] studied entropy generation and heat transfer simulation of Al_2O_3 and carbon nanotubes-based hybrid nanofluids in a square shape enclosure, heat transfer rates increase from 8.20% to 17.60% when the solid-volume fraction was 0.05 in case of carbon nanotubes and heat transfer rates increases from 8.20% to 12.40% when Al_2O_3 suspended nanofluid with the volume fraction 0.050 was used. Soomro et al. [14] reported the findings of the study of mixed convection heat transfer within a lid-driven semi-circular shaped cavity and revealed that raising the Richardson number reduces heat transfer rates while increasing the Hartman number increases heat transfer rates. In a wavy-shaped cavity, non-Newtonian hybrid nanofluid was numerically examined by Hussain et al. [15]. The results of the study revealed optimum heat transfer rates are achieved with pseudo-plastic hybrid nanofluids when the Rayleigh number is higher and Hartmann number is lower. The study carried out by Shorbagy et al. [16] on the effect of fin thickness on mixed convection of hybrid nanofluid suggests that increasing the concentration of hybrid nanofluids in the base fluid increases the heat transfer rates. Vidhya et al. [17] studied the thermophysical properties of zinc/oxide hybrid nanofluid for heat transfer applications. Results suggested that while using hybrid nanofluids heat transfer coefficient is enhanced by 28.9% and thermal resistance is decreased by 4.07%. According to a study by Azmi et al. [18] on the thermal-hydraulic performance of a hybrid nanofluid in a tube with wire coil inserts, the performance of the fluid is enhanced by the larger concentration of each nanoparticle, which accelerates heat transfer. Thermal radiation, heat creation, and chemical reactions were investigated on hybrid nanofluid in a study on $Ag-Cu/water$ hybrid nanofluid heat transfer enhancement by Hayat et al. [19]. The results suggest that in the presence of these parameters, the heat transfer rate of a hybrid nanofluid is greater than that of a conventional nanofluid. Soomro et al. [20] conducted a numerical analysis of the MHD $Al_2O_3-Cu/water$ hybrid nanofluid's heat transmission capabilities over an inclined surface. The results revealed that heat transfer is increased by using a hybrid nanofluid in comparison to simple nanofluid. A study of nanofluids inside a triangle-shaped cavity of mixed convection was conducted by Khadija et al. [21] in which unsteady behavior of different nanofluids was carried. Results suggested that the higher aspect ratio results in a higher Nusselt number. Moreover, Fe_3O_4-EO provides higher results of heat transfer as compared to $Fe_3O_4-H_2O$. In one of the studies conducted by Massoudi et al. [22] on diamond-water nanofluid to study the effect of MHD natural convection and thermal radiation inside a trapezoid cavity, results show that using nanofluids with high shape factor improves the heat transfer rates. A comparative study on water and kerosene filled $Fe_3O_4-MWCNT$ hybrid nanofluid were carried by Thirumalaisa et al. [23] inside a porous square enclosure, 5% of nanoparticles is added in water and kerosene, results revealed that higher mean heat transfer rate is achieved with kerosene based nanofluids. Soomro et al. [24] examined the thermal performance of MHD considering triangle-shaped chamber with a circular barrier which has mixed convection flow. Heat transfer increases with an increase in the Richardson number and decreases with a rise in the Hartmann number, according to a study that analyzed several physical characteristics including the Reynolds number, Richardson number, and Hartmann number.

Mohammad et al. [25] natural convection was investigated in a wavy cage using hybrid nanofluid and heated cylinder, study shows that by increase in Hartmann number convective flow is decreased and up to 25% increase in heat transfer while using nanofluids. Numerical study on MHD convective flow using hybrid-nanofluid in an elliptic porous enclosure were carried by Shehzad et al. [26] he suggested that great heat transfer and high Rayleigh number is achieved while using nanofluids. Hossain et al. [27] carried work on MHD natural convection flow using nanofluid inside porous trapezoidal cavity with high temperature triangular obstacle, numerical experiments suggests that flow is stronger when Ra and Da is higher and heat transfer rates also depends upon aspect ratio. Inside a triangular cavity that is slightly heated at the bottom, a study is being conducted on the natural convection of nanofluids by Khan et al. [28] It has been found that as Nanoparticles' Rayleigh number and solid-volume fraction increase, local and average Nusselt numbers also rise. Thermal conductivity's influence on heat transmission was studied by Khadim et al. [29] using Natural convection of a hybrid nanofluid numerically analyzed inside a wavy enclosure. It was discovered that heat transfer increases as thermal conductivity increases up to a value of 0.04. In one of the studies carried by Sreedevi et al. [30] to observe the effects of the magnetic field and heat radiation on natural convection using T_iO_2 nanoparticles inside a square cavity. Therefore, the primary goal of this study is to numerically analyze a partially heated trapezoid cavity for heat transfer characteristics of hybrid nanofluids. This cavity has a heat obstacle in the center, adiabatic side walls and a heated bottom wall while the top wall is kept at a lower temperature. Isotherms, the Nusselt number, and streamlines are used to display temperature, heat transfer rates, as well as fluid flow. For further useful reading, refer to the articles [31-34].

In this piece of work, the heat transfer rate is analyzed upon using hybrid nanofluids with different base fluids inside a partially heated trapezoidal shape cavity with heated obstacle at the center. The objective is to attain the augmentation in heat transfer due to use of various hybrid nanofluids. The paper is distributed into various sections. Section 1 is devoted to the importance and related work reported in the past. The mathematical framework of the problem is presented in the section 2. A numerical solution procedure is explained in section 3. The obtained results are discussed in the section 4. The conclusion of the presented study is depicted in section 5. Finally, all the cited references are listed in the end of article in the references section.

2. Mathematical Formulation

In this work, a numerical study of the steady, two-dimensional, incompressible flow of viscous fluid inside a partially heated trapezoidal cavity with a heated obstacle at the centre is carried out. The cavity is filled with hybrid nanofluids of two types of nanoparticles: Silver (Ag) and Magnesium Oxide (MgO) suspended into three types of fluids: water, kerosene, and engine oil. The cavity is partially heated at the bottom, kept at comparatively at low temperature at side inclined walls, and adiabatic top wall. The geometry of the cavity can be seen in Fig. 1. The cavity is subject to a transverse magnetic field normal to the bottom heated boundary. Considering the low Reynolds number such that the induced magnetic field is neglected in comparison to an applied magnetic field. Moreover, viscous dissipation effects are also neglected. The governing equations for above considered criteria are given as below [35].

$$\frac{\partial u}{\partial x}+\frac{\partial v}{\partial y}=0, \tag{1}$$

$$u\frac{\partial u}{\partial x}+v\frac{\partial u}{\partial y}=-\frac{1}{\rho_{hnf}}\frac{\partial p}{\partial x}+\nu_{hnf}\left(\frac{\partial^2 u}{\partial x^2}+\frac{\partial^2 u}{\partial y^2}\right) \tag{2}$$

$$u\frac{\partial v}{\partial x}+v\frac{\partial v}{\partial y}=-\frac{1}{\rho_{hnf}}\frac{\partial p}{\partial y}+\nu_{hnf}\left(\frac{\partial^2 v}{\partial x^2}+\frac{\partial^2 v}{\partial y^2}\right)$$
$$-\frac{\sigma_{hnf}}{\rho_{hnf}}B_0^2 v+g\beta_{hnf}(T^*-T_c^*) \tag{3}$$

$$u\frac{\partial T^*}{\partial x}+v\frac{\partial T^*}{\partial y}=\alpha_{hnf}\left(\frac{\partial^2 T^*}{\partial x^2}+\frac{\partial^2 T^*}{\partial y^2}\right) \tag{4}$$

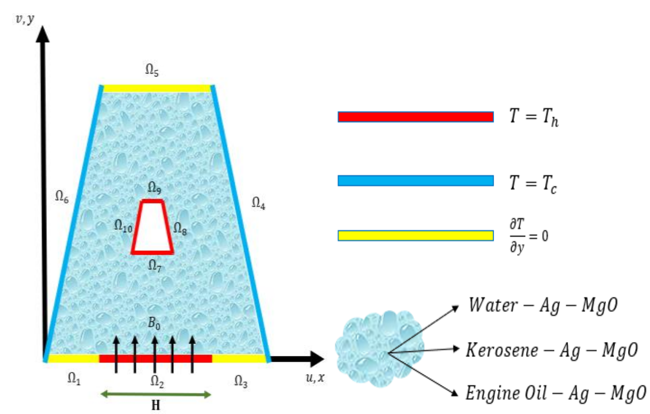

Fig. 1. Graphical Representation of the Geometry

where p is the pressure, g is the acceleration due to gravity, T^* is the temperature of the fluid, u and v are the respective velocities along the x and y directions. Thermophysical properties of hybrid nanofluid are density ρ_{hnf}, dynamic viscosity $\nu_{hnf}\left(=\frac{\mu_{hnf}}{\rho_{hnf}}\right)$, kinematic viscosity μ_{hnf}, electric conductivity σ_{hnf}, thermal expansion coefficient β_{hnf}, thermal diffusivity $\alpha_{hnf}\left(=\frac{k_{hnf}}{(\rho Cp)_{hnf}}\right)$, thermal conductivity k_{hnf}, and specific heat capacity $\left(c_p\right)_{hnf}$. These thermophysical properties of base fluids (water, kerosene, and engine oil) and nanoparticles (Ag and MgO) are given by the following nano relations:

$$\frac{\mu_{hnf}}{\mu_f} = (1-\phi)^{2.5},$$
$$\frac{\rho_{hnf}}{\rho_f} = (1-\phi) + \phi_1\left(\frac{\rho_1}{\rho_f}\right) + \phi_2\left(\frac{\rho_2}{\rho_f}\right),$$
$$\frac{(\rho\beta)_{hnf}}{(\rho\beta)_f} = (1-\phi) + \phi_1\left(\frac{(\rho\beta)_1}{(\rho\beta)_f}\right) + \phi_2\left(\frac{(\rho\beta)_2}{(\rho\beta)_f}\right),$$
$$\frac{\sigma_{hnf}}{\sigma_f} = 1 + \frac{3\phi\left(\sigma_1\phi_1+\sigma_2\phi_2-\sigma_f(\phi_1+\phi_2)\right)}{(\phi_1\sigma_1+\phi_2\sigma_2+2\phi\sigma_f)-\phi(\sigma_f(\phi_1\sigma_1+\phi_2\sigma_2)-\sigma_f(\phi_1+\phi_2))},$$
$$\frac{k_{hnf}}{k_f} = \frac{(\phi_1k_1+\phi_2k_2+2\phi k_f)+2\phi(\phi_1k_1+\phi_1k_2)-2\phi^2k_f}{(\phi_1k_1+\phi_2k_2+2\phi k_f)-\phi(\phi_1k_1+\phi_1k_2)+\phi^2k_f},$$
$$\frac{(\rho c_p)_{hnf}}{(\rho c_p)_f} = (1-\phi_1-\phi_2) + \phi_1\left(\frac{(\rho c_p)_1}{(\rho c_p)_f}\right) + \phi_2\left(\frac{(\rho c_p)_2}{(\rho c_p)_f}\right), \tag{5}$$

where $\phi=\phi_1+\phi_2$ represents the total volume of nanoparticles fraction, and $(*)_f$, $(*)_1$ and $(*)_2$ respectively shows the property of base fluid, Ag nanoparticles and MgO nanoparticles, which are given in Table 1. The velocity and temperature conditions imposed on the walls of the trapezoid cavity are given as follows:

$$\begin{array}{ll} \textit{at heated walls} & \Omega_2,\Omega_7,\Omega_8,\Omega_9,\Omega_{10} \\ \textit{at cold walls} & \Omega_4,\Omega_6 \\ \textit{at adiabatic walls} & \Omega_1,\Omega_3,\Omega_5 \end{array}$$
$$\begin{array}{c} u=0, v=0, T^*=T_h^* \\ u=0, v=0, T^*=T_c^* \\ u=0, v=0, \frac{\partial T^*}{\partial y}=0 \end{array} \tag{6}$$

Using the following transformation variables:

$$X=\frac{x}{H}, Y=\frac{y}{H}, U=\frac{uH}{\alpha_f}, V=\frac{vH}{\alpha_f}, P=\frac{pH^2}{\rho_f\alpha_f^2}, T=\frac{T^*-T_c^*}{T_h^*-T_c^*},$$
$$\nu_f=\frac{\mu_f}{\rho_f}, Ra=\frac{\beta_f(T_h^*-T_c^*)H^3}{\nu_f\alpha_f}, Ha=B_0H\sqrt{\frac{\sigma_f}{\rho_f\nu_f}}, Pr=\frac{\nu_f}{\alpha_f}. \tag{7}$$

Table 1

Thermophysical characteristics of water and nanoparticle [36-37]

Properties	ρ	C_p	k	$\beta\times10^{-5}$	σ	μ	Pr
Water	997.1	4,179	0.613	21	5.5×10^{-6}	0.001003	6.8377
Kerosene	783	2,090	0.149	99	6.0×10^{-10}	0.00164	23.004
Engine Oil	888.23	1,880.3	0.145	70	23.004	0.8451	10958.9
Ag	10,500	235	429	1.89	8.1×10^{-4}	---	---
MgO	3,560	955	45	1.05	8×10^{-4}	---	---

where H is the length of heated bottom boundary, Ra is the Rayleigh number, Ha is the Hartmann number, and Pr is the Prandtl number. Incorporating variables in Eq. 7, the Eq. 1-4 may be written in the non-dimensional form as:

$$\frac{\partial U}{\partial X}+\frac{\partial V}{\partial y}=0, \tag{8}$$

$$U\frac{\partial U}{\partial X}+V\frac{\partial V}{\partial y}=-\frac{\rho_f}{\rho_{hnf}}\frac{\partial P}{\partial X}+\Pr\frac{\nu_{hnf}}{\nu_f}\left(\frac{\partial^2U}{\partial X^2}+\frac{\partial^2U}{\partial Y^2}\right) \tag{9}$$

$$U\frac{\partial V}{\partial X}+V\frac{\partial V}{\partial y}=-\frac{\rho_f}{\rho_{hnf}}\frac{\partial P}{\partial Y}+\Pr\frac{\nu_{hnf}}{\nu_f}\left(\frac{\partial^2V}{\partial X^2}+\frac{\partial^2V}{\partial Y^2}\right)$$
$$-Ha^2\Pr V+\frac{(1-\phi)(\rho\beta)_f+\phi_1(\rho\beta)_1+\phi_2(\rho\beta)_2}{\rho_{hnf}\beta_f}RaPrT \tag{10}$$

$$U\frac{\partial T}{\partial X}+V\frac{\partial T}{\partial Y}=\frac{\alpha_{hnf}}{\alpha_f}\left(\frac{\partial^2T}{\partial X^2}+\frac{\partial^2T}{\partial Y^2}\right) \tag{11}$$

With the boundary conditions

$$\begin{array}{ll} \textit{at heated walls} & \Omega_2,\Omega_7,\Omega_8,\Omega_9,\Omega_{10} \\ \textit{at cold walls} & \Omega_4,\Omega_6 \\ \textit{at adiabatic walls} & \Omega_1,\Omega_3,\Omega_5 \end{array}$$
$$\begin{array}{c} U=0, V=0, T=1 \\ U=0, V=0, T=0 \\ U=0, V=0, \frac{\partial T}{\partial Y}=0 \end{array} \tag{12}$$

Moreover, the heat transfer rate at the bottom heated boundary, given by the local Nusselt number, is described as:

$$Nu_{Loc}=-\frac{k_{hnf}}{k_f}\frac{\partial T}{\partial Y} \tag{13}$$

whereas, the average Nusselt number is given by

$$Nu_{Avg}=\frac{1}{H}\int_H Nu_{Loc}\,dX \tag{14}$$

3. Solution Procedure

The governing Eq. 8-11 along with the associated boundary conditions (12) are solved using the well-known numerical method called Finite Element Method (FEM) adopting Galerkin approach. The fundamentals and procedure about the method is well explained by Dechaumphai [38] and Taylor and Hood [39]. The space domain of the cavity is discretised by the finite number of non-uniform triangular mesh elements (see Fig. 2(a)). Moreover, at the critical boundary positions like, along the heated boundaries, comparatively denser mesh is utilized. The pressure term P may be eliminated from the Eq. 9 and Eq. 10 by the following continuity constraint equation:

$$P = -\gamma \left(\frac{\partial U}{\partial X} + \frac{\partial V}{\partial Y} \right) \quad (15)$$

Using Eq. 15, the Eq. 9-10 reduces to

$$U \frac{dU}{dX} + V \frac{\partial U}{\partial Y} = \gamma \frac{\rho_f}{\rho_{hnf}} \frac{\partial}{\partial X} \left(\frac{\partial U}{\partial X} + \frac{\partial V}{\partial Y} \right) + Pr \frac{\nu_{hnf}}{\nu_f} \left(\frac{\partial^2 U}{\partial X^2} + \frac{\partial^2 U}{\partial Y^2} \right) \quad (16)$$

$$U \frac{\partial U}{\partial X} + V \frac{\partial U}{\partial y} = \gamma \frac{\rho_f}{\rho_{hnf}} \frac{\partial}{\partial Y} \left(\frac{\partial U}{\partial X} + \frac{\partial V}{\partial Y} \right) + Pr \frac{\nu_{hnf}}{\nu_f} \left(\frac{\partial^2 V}{\partial X^2} + \frac{\partial^2 V}{\partial Y^2} \right) - Ha^2 \, \mathrm{Pr}\, V + \frac{(1-\phi)(\rho\beta)_f + \phi_1 (\rho\beta)_1 + \phi_2 (\rho\beta)_2}{\rho_{hnf} \beta_f} RaPrT \quad (17)$$

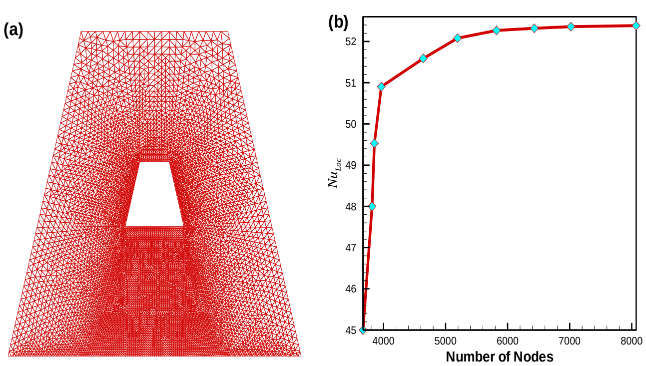

Fig. 2. (a) Triangular mesh and (b) mesh sensitivity curve

Table 2

Comparison of the work of Khanafer et al [40] and Davis [41] with present results

Ra	Khanafer et al.	De Vahl Davis	Present Results
10^3	1.118	1.118	1.13073
10^4	2.245	2.243	2.26744
10^5	4.522	4.519	4.58512
10^6	8.826	8.799	8.83413

For large values of γ ($\gamma = 10^7$) the continuity equation is satisfied. Mesh sensitivity curve is presented in Fig. 2(b). It depicts that the number of nodes greater than or equal to 7500 is suitable to get the results with accuracy. The validity of the present code is carried out by performing the simulation on the mathematical model reported by Khanafer et al. [40] and De Vahl Davis [41]. The strong agreement between the results, presented in Table 2, shows the applicability of presented results.

4. Results and Discussion

Natural convection flow and heat transfer inside a hybrid nanofluid filled partially heated trapezoidal cavity is investigated in this study. For numerical simulation, the Finite Element Method (FEM) with Galerkin approach is utilized. The important physical parameters under consideration are nanoparticles volume fraction ϕ ($0 \leq \phi \leq 0.2$), Rayleigh number Ra ($10^5 \leq Ra \leq 10^7$), and Hartman number Ha ($0 \leq Ha \leq 100$). Water, kerosene, and engine oil containing $Ag - MgO$ nanoparticles are among the nanofluid choices. The results are presented in the form of heat transfer rate using Nusselt number both locally and average, temperature profile along mean path, temperature distribution using isotherms, and flow distribution using streamlines. The goal of this research is to determine the primary parameters impacting heat transfer. Fig.s 3-9 demonstrate how the important factors affect flow distribution, heat distribution, and heat transfer rate. The initial experiment is performed by calculating the local and average heat transfer rate along the bottom heated boundary for different base fluids suspended in Ag and MgO nanoparticles which is presented in Fig. 3(a)-(b). The profiles trend clearly depicts that compared to $water - Ag - MgO$ and $Kerosene - Ag - MgO$ hybrid nanofluids, the heat transfer rate using $engine\ oil - Ag - MgO$ hybrid nanofluid is maximum. Therefore, the rest of the simulation is performed using $engine\ oil - Ag - MgO$ hybrid nanofluid and the detailed analysis is presented in the subsequent paragraphs.

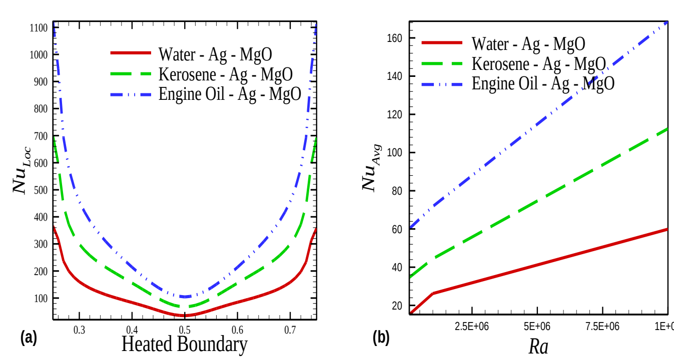

Fig. 3. Average Nusselt number for various hybrid nanofluids

4.1 Effect Of Increasing Nanofluid Volume-Fraction

The temperature distribution of nanofluids is represented by isotherms in Fig. 4(a)-(c), which illustrate the impact on isotherms when the volume fraction of nanoparticles grows. The bottom of the hollow and the inner trapezoidal cylinder are partially heated. The trend of the isotherms shows that the temperature distribution of the fluid tends to rise as the nanoparticle volume percentage increases. This is owing to nanoparticles' increased heat conductivity. The fluid motion trajectories, on the other hand, are indicated by streamlines as the impact of nanoparticle volume fraction increase (Fig.4(d)-(f)). It is clear that as the volume percentage of nanoparticles increases, so does the strength of the streamlines.

The effects of increasing the nanoparticle volume percent on the temperature along the vertical mean position and heat transfer rate along bottom heated border are shown in Fig.5. Fig. 5(a) depicts the temperature distribution at the mean vertical position. The profiles clearly illustrate that the temperature of the fluid increases along the bottom mean path due to an increase in the nanoparticle volume percentage. The temperature, on the other hand, tends to drop when the nanoparticle volume fraction increases along upper mean path. The heat transfer rate along the heated length of the trapezoidal cavity is depicted in Fig. 5(b). The graph clearly shows that the heat transmission rate is greatest towards the extreme ends of the heated length. Furthermore, when the volume percentage of nanoparticles increases, the heat transmission rate decreases.

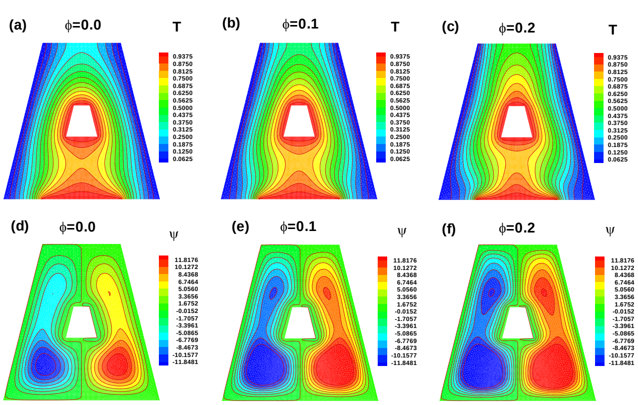

Fig. 4. Isotherms and streamlines under the effects of nanoparticles volume fraction when $Ra = 10^6$ and $Ha = 50$

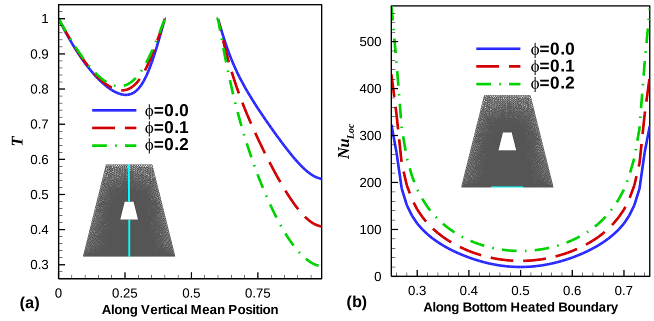

Fig. 5. Temperature and Nusselt number profiles under the effects of nanoparticles volume fraction when $Ra = 10^6$ and $Ha = 50$

4.2 Effect of Increasing Rayleigh Number

The temperature distribution as a function of the Rayleigh number Ra is represented in Fig.6(a)-(c). Fig. 6(a) illustrates that for low Rayleigh numbers, isotherms are smooth, indicating that conduction flow is dominant. The thermal boundary layer thickens as it approaches the cavity's side corners and top portion. Overall, heat transport occurs by conduction. Furthermore, as the Rayleigh number $Ra = 10^6$ is raised, buoyant forces are taken into consideration, and the isotherms becomes non smooth along the heated boundaries. At $Ra = 10^7$, strong isotherms demonstrate the dominance of buoyant force. Due to high buoyancy effects, the isotherms become turbulent and the cavity top section becomes heated. That is, heat transport occurs as a result of convection.

The streamlines for the nanofluid flow are shown in Fig. 6(d)-(f) for various increasing Rayleigh numbers. The streamlines are dispersed into two symmetrical boluses, one on either side of the cavity. This is owing to the boundary conditions that have been established. The fluid heats up and rises in the centre, then cools down at the side walls, causing such circulation. The intensity of streamlines is modest at low Reynolds number $Ra = 10^5$, indicating that heat transmission is due to conduction. The strength of streamlines rises as the Rayleigh number increases. In comparison to $Ra = 10^5$, where buoyancy effects are less important, streamlines dominate the whole cavity at $Ra = 10^6$, demonstrating the dominance of convective heat transmission. At $Ra = 10^5$, 10^6 and 10^7 the absolute value of the stream function reaches maximum values of 1.1457, 38.4437, and 92.4334, respectively.

The temperature T changes owing to the range of Rayleigh numbers Ra values are depicted in Fig.7(a). The results are computed along the vertical mean position. It depicts the shift in fluid temperature from (0,0.5) to (0.5,1). It can be observed that the temperature tends to drop as the Rayleigh number grows from 0 to 0.5, but it increases when the Rayleigh number increases from 0.5 to 1. The variation in the local Nusselt number Nu_{Loc} owing to the different range of Rayleigh numbers Ra is shown in Fig.7(b). The graphic clearly shows that the heat transmission rate is greatest at the extreme ends of the heated length. Furthermore, as the Rayleigh number grows, so do the heat transfer rates, with the exception of the midway, where the Rayleigh number has no influence on heat transfer rates.

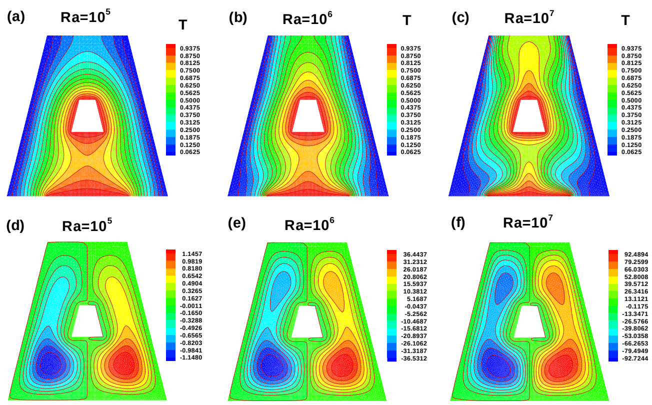

Fig. 6. Isotherms and streamlines for the values of Rayleigh number when $\phi = 0.2$ and $Ha = 50$

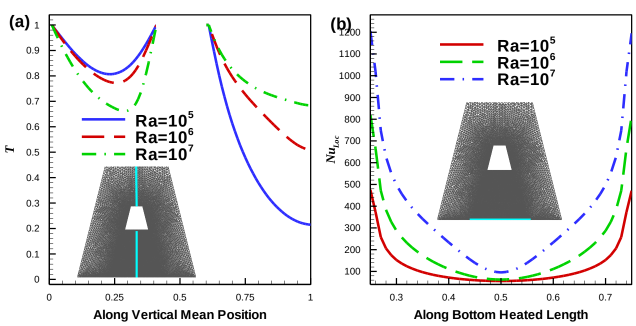

Fig. 7. Temperature and Nusselt number profiles under the variation effects of Rayleigh number when $\phi = 0.2$ and $Ha = 50$

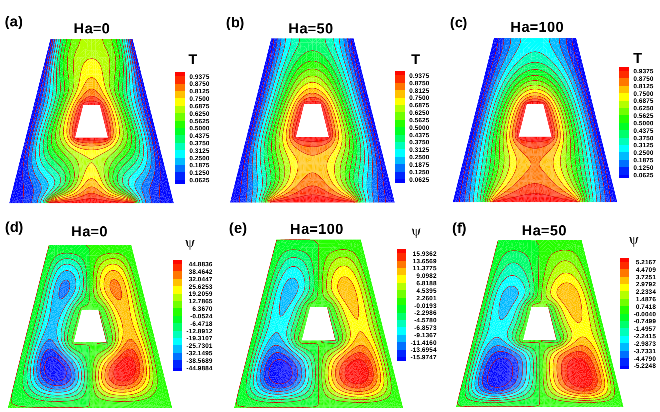

Fig. 8. Isotherms and streamlines under the effects of Hartmann number when $\phi = 0.2$ and $Ra = 10^6$

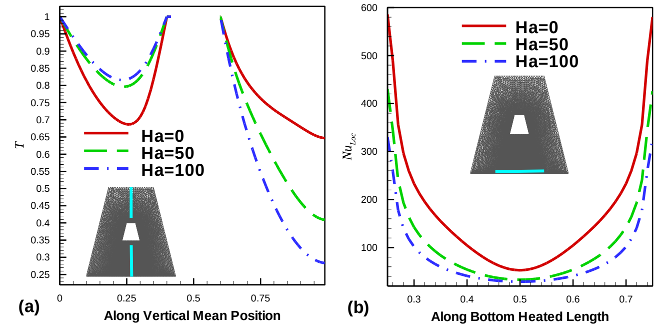

Fig. 9. Temperature and Nusselt number profiles under the effects of Hartmann number when $\phi = 0.2$ and $Ra = 10^6$

4.3 *Effect Of Increasing Hartmann Number*

Fig. 8(a)-(c) show the variance in the temperature distribution for different values of the Hartmann number Ha. The Hartmann number is a dimensionless quantity used in magnetohydrodynamics to represent the relative relevance of magnetic force to viscous forces in a conducting flow subjected to magnetic field effects. Fig. 8(a) shows that for low Hartmann numbers, isotherms at the top are turbulent, as opposed to Fig. 8(b) and 8(c). The thickness of the thermal boundary layer rises towards the top portion and side corners of the cavity. Furthermore, raising the Hartmann number to $Ha = 50$ allows viscous forces to be considered, but buoyancy forces still dominate. Isotherms at $Ha = 100$ reveal the dominance of viscous forces. Because of the high viscous forces, the streamlines become smooth in the top section of the cavity.

The streamlines for the nanofluids are shown in Fig.8(d)-(f) for various Hartmann numbers. The streamlines are spreading into two symmetrical boluses on the cavity's left and right sides. This is due to enforced boundary constraints. The strength of the streamlines is minimal for high Hartmann number $Ha = 100$, indicating that heat transmission is due to conduction flow. The strength of streamlines rises as the Hartmann number falls. In comparison to $Ha = 100$, where buoyancy effects are less significant, streamlines occupy the whole cavity at $Ha = 0$, demonstrating the dominance of convective heat transmission. Absolute values of stream functions are 44.88, 15.93, and 5.21 for $Ha = 0,\ 50,$ and 100, respectively.

The change in temperature T caused by different Hartmann number Ha values is seen in Fig.9(a). The values are computed along the mean position. The graph shows that from 0 to 0.5, temperature tends to rise as the Hartmann number rises, but from 0.5 to 1, temperature tends to fall as the Hartmann number rises. The variation in the Local Nusselt number Nu_{Loc} owing to different Hartmann number Ha values is shown in Fig.9(b). The results are proportional to the heated length of the trapezoidal cavity. The graphs clearly shows that the heat transfer rate is highest at the heated length's extreme ends. Furthermore, when the Hartmann number grows, heat transfer rates tend to decrease, with the exception of the middle, where the Hartmann number has no influence on heat transfer rates.

5. Conclusion

The behaviour of $water - Ag - MgO$, $Kerosene - Ag - MgO$, and $Engine\ Oil - Ag - MgO$ hybrid nanofluids within a partially heated trapezoidal cavity containing a heated trapezoidal cylinder is investigated numerically in this paper. To solve the governing equations, the Finite Element Method is applied. The effects of Rayleigh number (Ra), nanoparticle volume percentage (ϕ), and Hartmann number (Ha) on flow and heat distribution as well as on heat transfer rate are considered. The study's findings reveal that among the considered hybrid nanofluids, engine oil-based hybrid nanofluid works best as it provides enhanced heat transfer rate. At low Rayleigh numbers, heat transfer primarily occurs through conduction, while at high Rayleigh numbers, convection becomes the dominant heat transfer mechanism. Increasing the volume percentage of nanoparticles improves average heat transfer rates. Higher values of the Hartmann number equate to a stronger magnetic field, resulting in less fluid movement.

6. Declaration of Competing Interests

The authors declare that they have no known competing financial interests or personal relationships that could have appeared to influence the work reported in this paper.

7. Acknowledgment

Princess Nourah bint Abdulrahman University through researchers supporting Project number (PNURSP2023R154), Princess Nourah bint Abdulrahman University, Riyadh, Saudi Arabia.

8. References

[1] F.P. Incropera, “Convection heat transfer in electronic equipment cooling,” ASME journal of heat and mass Transfer, vol. 110, pp. 1097-1111, 1988, doi.org/10.1115/1.3250613

[2] M. Roksland, T.A. Basmoen, and D. Sui, “Geothermal energy extraction from abandoned wells,” Energy Procedia, vol. 105, pp. 244-249, 2017, doi.org/10.1016/j.egypro.2017.03.309

[3] M. Muneeshwaran, G. Srinivasan, P. Muthukumar, and C.C Wang, “Role of hybrid-nanofluid in heat transfer enhancement: A review,” International Communications in Heat and Mass Transfer, vol. 225, pp. 105341, 2021, https://doi.org/10.1016/j.icheatmasstransfer.2021.105341

[4] B. Bakthavatchalam, K. Habib, R. Saidur, B.B. Saha, and K. Irshad, “Comprehensive study on nanofluid and nanofluid for heat transfer enhancement,” A review on current and future perspective, Journal of Molecular Liquids, vol. 305, pp. 112787, 2020, doi.org/10.1016/j.molliq.2020.112787

[5] F. M. Oudina and I. Chabani, “Review on nano-fluids applications and heat transfer enhancement techniques in different enclosures,” Journal of nanofluids, vol. 11, pp. 155-168, 2022, doi.org/10.1166/jon.2022.1834

[6] S.U. Choi, and J.A. Eastman, “Enhancing thermal conductivity of fluids with nanoparticles,” Argonne National Lab, vol. 231, pp. 99-103, 1995.

[7] S.O. Giwa, M. Sharifpur, M.H. Ahmadi, and J.P. Meyer, “A review of magnetic field influence on natural convection heat transfer performance of nanofluids in square cavities,” Journal of Thermal Analysis and Calorimetry, vol. 145, pp. 2581-2623, 2021, doi.org/10.1007/s10973-020-09832-3

[8] R.U. Haq, F.A. Soomro, and Z. Hammouch, “Heat transfer analysis of CuO-water enclosed in a partially heated rhombus with heated square obstacle,” International Journal of Heat and Mass Transfer, vol. 118, pp. 773-784, 2018, doi.org/10.1016/j.ijheatmasstransfer.2017.11.043

[9] R.U. Haq, S.N. Kazmi, and T. Mekkaoui, “Thermal management of water based SWCNTs enclosed in a partially heated trapezoidal cavity via FEM,” International Journal of Heat and Mass Transfer, vol. 112, pp. 972-984, 2017, doi.org/10.1016/j.ijheatmasstransfer.2017.05.041

[10] S. Alqaed, J. Mustafa, and M. Sharifpur, “Numerical investigation and optimization of natural convection and entropy generation of alumina/H_2O nanofluid in a rectangular cavity in the presence of a magnetic field with artificial neural networks,” Engineering Analysis with Boundary Elements, vol. 140, pp. 507-518, 2022, doi.org/10.1016/j.enganabound.2022.04.034

[11] M.A. Alomari, K.A. Farhany, A.L. Hashem, M.F. Al-Dawody, and F. Redouane, "Numerical study of MHD natural convection in trapezoidal enclosure filled with (50%MgO-50%Ag/Water) hybrid nanofluid: heated sinusoidal from below," International Journal of Heat and Technology, vol. 39, pp. 1271-1279, 2021, iieta.org/journals/ijht

[12] M. Ghalambaz, A. Doostani, E. Izadpanahi, and A.J. Chamkha, "Conjugate natural convection flow of Ag-MgO/water hybrid nanofluid in a square cavity," Journal of Thermal Analysis and Calorimetry, vol. 139, pp. 2321-2336, 2020, doi.org/10.1007/s10973-019-08617-7

[13] P. Sreedevi and P.S. Reddy," Entropy generation and heat transfer analysis of alumina and carbon nanotubes-based hybrid nanofluid inside a cavity," Physica Scripta, vol. 96, no.8, pp. 085210, 2021, doi.org/10.1088/1402-4896/ac0077

[14] F.A. Soomro, M. Hamid, S.T. Hussain, and R.U. Haq, "Constructional design and mixed convection heat transfer inside lid-driven semicircular cavity," The European Physical Journal Plus, vol. 137, pp. 781, 2022, https://doi.org/10.1140/epjp/s13360-022-03009-7

[15] S. Hussain, T. Tayebi, T. Armaghani, A.M. Rashad, and H.A. Nabwey, "Conjugate natural convection of non-Newtonian hybrid nanofluid in wavy-shaped enclosure," Applied Mathematics and Mechanics, vol. 43, pp. 447-466, 2022, doi.org/10.1007/s10483-022-2837-6

[16] M.A. El-Shorbagy, E.A. Algehyne, M. Ibrahim, V. Ali, and R. Kalbasi, "Effect of fin thickness on mixed convection of hybrid nanofluid exposed to magnetic field-Enhancement of heat sink efficiency," Case Studies in Thermal Engineering, vol. 26, pp. 101037, 2021, doi.org/10.1016/j.csite.2021.101037

[17] R. Vidhya, T. Balakrishnan, and B. Suresh Kumar, "Investigation on thermophysical properties of zinc oxide nanofluid for heat transfer applications," Materials Today: Proceedings, vol. 58, pp. 789-794, 2022, doi.org/10.1016/j.matpr.2021.09.008

[18] W.H. Azmi, K.A. Hamid, A.I. Ramadhan, and A.I.M. Shaiful, "Thermal hydraulic performance for hybrid composition ratio of TiO_2-SiO_2 nanofluids in a tube with wire coil inserts," Case Studies in Thermal Engineering, vol. 25, pp. 100899, 2021, doi.org/10.1016/j.csite.2021.100899

[19] T. Hayat, and S. Nadeem, "Heat transfer enhancement with Ag-CuO/water hybrid nanofluid," Results in Physics, vol. 7, pp. 2317-2324, 2017, doi.org/10.1016/j.rinp.2017.06.034

[20] F.A. Soomro, M. Usman, S.E. Sapa, M. Hamid, and R.U. Haq, "Numerical study of heat transfer performance of MHD $Al_2O_3 - Cu/water$ hybrid nanofluid flow over inclined surface," Archive of Applied Mechanics, vol. 92, pp. 2757-2765, 2022, doi.org/10.1007/s00419-022-02214-1

[21] A.K. Al-Hussani, M.S. Alam, and M.M. Rahman, "Numerical simulations of hydromagnetic mixed convection flow of nanofluids inside a triangular cavity on the basis of a two-component nonhomogeneous mathematical model," Fluid Dynamics and Material Processing, vol. 17, pp. 1-20, 2021, doi.org/10.32604/fdmp.2021.013497

[22] M.D. Massoudi and M.B.B. Hamida, "MHD natural convection and thermal radiation of diamond water nanofluid around rotating elliptical baffle inside inclined trapezoidal cavity," The European Physical Journal Plus, vol. 135, pp. 902, 2020, doi.org/10.1140/epjp/s13360-020-00921-8

[23] K. Thirumalaisamy, S. Ramachandran, V. R. Prasad, O. A. Beg, H. Leung, F. Kamalov, and R. P. Selvam, "Comparative heat transfer analysis of electroconductive $Fe_3O_4 - MWCNT - water$ and $Fe_3O_4 - MWCNT - kerosene$ hybrid nanofluids in a square porous cavity using the non-Fourier heat flux model," Physics of Fluids, vol. 34, pp. 122016, 2022, doi.org/10.1063/5.0127463

[24] F.A. Soomro, R.U. Haq, E.A. Algehyne, and I. Tlili, "Thermal performance due to magnetohydrodynamics mixed convection flow in a triangular cavity with circular obstacle," Science Direct, vol. 31, pp. 101702, 2020, https://doi.org/10.1016/j.est.2020.101702

[25] M.M. Ali, R. Akhter, and M.A. Alim, "Hydromagnetic natural convection in a wavy-walled enclosure equipped with hybrid nanofluid and heat generating cylinder," Science Direct, vol. 60, pp. 5245-5264, 2021,

doi.org/10.1016/j.aej.2021.04.059

[26] S.A. Shehzad, M. Sheikholeslami, T. Ambreen, and A. Shafee, “Convective MHD flow of hybrid-nanofluid within an elliptic porous enclosure,” Science Direct, vol. 384, pp. 126727, 2020, doi.org/10.1016/j.physleta.2020.126727

[27] M.S. Hossain, M.A. Alim, and L.S. Andallah, “Numerical simulation of mhd natural convection flow within porous trapezoidal cavity with heated triangular obstacle,” International Journal of Applied and Computational Mathematics, vol. 6, pp. 166, 2020 doi.org/10.1007/s40819-020-00921-3

[28] Z.H. Khan, W.A. Khan, A.M.R. Elbaz, M. Qasim, S.O. Alharbi and L. Sun, “Natural convection in triangular fin-shaped Cavity with partially heated base using Nanofluid,” Z Angew Math Mech, vol. 101, pp. 202000306, 2021, doi.org/10.1140/epjp/s13360-022-03009-7

[29] H.T. Khadim, A.A. Manea, A.N. Al-Shamani, and T. Yusaf, “Numerical analysis of hybrid nanofluid natural convection in a wavy walled porous enclosure Local thermal non-equilibrium model,” International Journal of Thermo Fluids, vol. 15, pp. 100190, 2022, doi.org/10.1016/j.ijft.2022.100190

[30] P. Sreedevi and P.S. Reddy, “Effect of magnetic field and thermal radiation on natural convection in a square cavity filled with TiO_2 nanoparticles using Tiwari-Das nanofluid model,” Alexandria Engineering Journal, vol. 61, pp. 1529-1541, 2022, doi.org/10.1016/j.aej.2021.06.055

[31] M. Hamid, Z.H. Khan, W.A. Khan, Z. Tian, “Natural convection inside a trapezoidal cavity under multidirectional magnetic impacts: Finite element characterization,” Physics of Fluids, vol. 35, pp. 093618, 2023, https://doi.org/10.1063/5.0167791

[32] Z.J. Song, Z.H. Khan, R. Ahmad, W.A. Khan, and Y. Wei, “Thermal analysis of ferromagnetic nanofluid flow in a channel over a dimpled cavity,” Journal of Magnetism and Magnetic Materials, vol. 573, pp. 170653, 2023, https://doi.org/10.1016/j.jmmm.2023.170653

[33] Z.H. Khan, W.A. Khan, M. Qasim, S.O. Alharbi, M. Hamid, and M. Du, “Hybrid nanofluid flow around a triangular-shaped obstacle inside a split lid-driven trapezoidal cavity,” European Physical Journal Special Topics, vol. 231, pp. 2749-2759, 2022, doi.org/10.1140/epjs/s11734-022-00607-5

[34] ZH Khan, M Usman, WA Khan, M Hamid, and RU Haq, “Thermal treatment inside a partially heated triangular cavity filled with Casson fluid with an inner cylindrical obstacle via FEM approach,” European Physical Journal Special Topics, vol. 231, pp. 2683-2694, 2022, doi.org/10.1140/epjs/s11734-022-00587-6

[35] Z.H. Khan, W.A. Khan, and M. Hamid, “Non-Newtonian fluid flow around a Y-shaped fin embedded in a square cavity,” Journal of Thermal Analysis and Calorimetry, vol. 143, pp. 573-585, 2021, doi.org/10.1007/s10973-019-09201-9

[36] M. Benzema, Y.K. Benkahla, N. Labsi, S.E. Ouyahia, and M. El Ganaoui, “Second law analysis of MHD mixed convection heat transfer in a vented irregular cavity filled with Ag-MgO/water hybrid nanofluid,” Journal of Thermal Analysis and Calorimetry, vol. 137, pp. 1113-1132, 2019, doi.org/10.1007/s10973-019-08017-x

[37] A. Hussanan, M.Z. Salleh, I. Khan, and S. Shafie, “Convection heat transfer in micropolar nanofluids with oxide nanoparticles in water, kerosene and engine oil,” Journal of Molecular Liquids, vol. 229, pp. 428-488, 2017, doi.org/10.1016/j.molliq.2016.12.040

[38] P. Dechaumphai and W. Kanjanakijkasem, A Finite Element Method for Viscous Incompressible Thermal Flows, ScienceAsia, vol. 25, pp. 165-172, 1999

[39] C. Taylor and P. Hood, “A numerical solution of the Navier-Stokes equations using finite element technique,” Computers and Fluids, vol. 1, pp. 73-89, 1973, doi.org/10.1016/0045-7930(73)90027-3

[40] K. Khanafer, K. Vafai, and M. Lightstone, Buoyancy-driven heat transfer enhancement in a two-dimensional enclosure utilizing nanofluids, International Journal of Heat and Mass Transfer, vol. 46, no. 19, pp. 3639-3653, 2003, doi.org/10.1016/S0017-9310(03)00156-X

[41] G.D.V. Davis, “Natural convection of air in a square cavity, a benchmark numerical solution,” International Journal of Numerical Methods in Fluids, vol. 3, pp. 249-264, 1962, doi.org/10.1002/fld.1650030305